J Mol Model (2015) 21: 90
DOI 10.1007/s00894-015-2630-4

ORIGINAL PAPER

Mechanistic insights from molecular dynamic simulation of Rv0045c esterase in *Mycobacterium tuberculosis*

Durairaj Sherlin · Sharmila Anishetty

Received: 21 October 2014 / Accepted: 22 February 2015 / Published online: 19 March 2015

Abstract Rv0045c is an esterase involved in lipid metabolism of *Mycobacterium tuberculosis*. It belongs to the α/β hydrolase family. In the current study, we performed sequence- and structure-based analysis of Rv0045c followed by molecular dynamics (MD) simulation for 100 ns to investigate conformational changes in the enzyme. Sequence analysis revealed that this enzyme is possibly a hormone-sensitive lipase. Further, through structural analysis, a putative catalytic tetrad containing "Ser-Asp-Ser-His" and residues involved in the formation of an oxyanion hole were identified. MD simulation of Rv0045c revealed a conformational transition from an open to a closed state. The active site pocket was found to be gated by four loops. The potential role of the cap domain and the mobile histidine is discussed. From the simulation, we see that the conformational changes mimic the different stages in the reaction mechanism of Rv0045c. These results support the hypothesis that free enzyme simulation encompasses all the conformations necessary for the different stages of catalysis. Our findings add to the growing knowledge of an important family of esterases in *Mycobacterium tuberculosis*.

Keywords Esterase · Catalytic tetrad · Conformational transition · Hormone-sensitive lipase · Histidine flipping

Electronic supplementary material The online version of this article (doi:10.1007/s00894-015-2630-4) contains supplementary material, which is available to authorized users.

D. Sherlin · S. Anishetty (✉)
Center for Biotechnology, Anna University, Chennai 600 025, India
e-mail: sharmi.anishetty@gmail.com

S. Anishetty
e-mail: s_anishetty@annauniv.edu

Introduction

Esterases and lipases play an important role in the pathogenicity of *Mycobacterium tuberculosis* and in latent tuberculosis (TB) infection. An enriched knowledge of the biology of these esterases is of high priority in research aimed at developing new approaches and therapeutics to fight TB. Esterases (EC 3.1.1.1) are lipolytic enzymes that can hydrolyze soluble fatty acid esters without interfacial activation [1]. On the basis of amino acid sequence homology and conserved motifs, esterases can be classified into three groups: choline esterases, lipases and hormone sensitive lipases (HSL) [2]. Among these, HSL are very important as they play a vital role in dormancy by acting as rate-limiting enzymes in the mobilization of fatty acids from stored lipids [3]. Members of the HSL family have a conserved catalytic triad, Ser-His-Asp, in which Ser is embedded in the conserved sequence Gly-X-Ser-X-Gly. They also harbor a characteristic highly conserved motif "HGGG" that contributes to the formation of an oxyanion hole, located about 70–100 amino acids upstream of the catalytic serine.

Ester hydrolysis takes place in four major steps: the substrate is bound to the active site serine yielding a tetrahedral intermediate that is stabilized by the catalytic His and Asp residues. The alcohol is then released and an acyl–enzyme complex is formed. Attack of a nucleophile (catalytic water) forms a second tetrahedral intermediate, which, after resolution, yields an ester and a free enzyme [4]. Each stage of catalysis involves structural rearrangement and changes in the conformational state of the enzyme. Although experimentally determined structures of various conformational states in different enzymes have become increasingly available, they provide only static pictures. Transition between conformational states plays an important role in the functional activity of enzymes,

and molecular dynamic (MD) simulations can aid in understanding them.

Rv0045c, which participates in ester/lipid metabolism in *M. tuberculosis*, was characterized as an esterase belonging to the α/β hydrolase family [5]. The crystal structure of Rv0045c showed that it contains two distinct structural domains: an α/β fold domain and an inserted cap domain; the active site was found to comprise of two residues Ser154 and His309 (Fig. 1a). The role of the cap domain in Rv0045c is not completely understood [6]. Being a serine hydrolase, Rv0045c is an important therapeutic target for treating TB infection. Molecular dynamics simulation of Rv0045c esterase was carried out with the objective of studying the conformational transitions and gaining insights into the domain movements of the enzyme.

Materials and methods

Sequence analysis

A multiple sequence alignment of Rv0045c with the members of the HSL family was carried out using the Clustal server available at http://www.ebi.ac.uk/Tools/msa/clustalw2/ and results were shaded using Boxshade server (http://www.ch.embnet.org/software/BOX_form.html). The sequences were edited for optimal alignment. The sequences used for alignment with *M. tuberculosis* Rv0045c (**GI 339717515**) are *Archaeoglobus fulgidus* carboxylesterase (**GI 17943077**), *Acinetobacter* esterase (**GI 34559428**), *Homo sapiens* HSL (**GI 21328446**), Pseudomonas B11-1 lipase (**GI 2853612**), *M. tuberculosis* CDC1551 esterase (**GI 15840511**), *M. tuberculosis* Lipy PE-family protein (**GI 15842668**), *Ralstonia solancearum* putative esterase/lipase (**GI 17545158**) and *M. tuberculosis* Rv1399c (**GI 81669984**).

Molecular docking studies

Docking studies were performed with the help of Autodock v4.2 [7]. Preparation of the receptor, ligand and grid was achieved using the MGL Autodock Tools package (ADT). The grid box was positioned around the catalytic triad and the oxyanion residues with a default grid spacing of 0.375 Å. We selected the genetic algorithm for ligand conformational searching. Interatomic contacts were analyzed with a cut-off distance of 0.25 Å using the What-if server [8] and visualized in Pymol [9].

Molecular dynamics simulation

The structure of Rv0045c esterase was retrieved from Protein Data Bank (PDBID: 3P2M). The structure had some missing residues (1–38 and 194–204). The region from 194–204 belongs to the cap domain region and was loop modelled using the modloop server [10] available at http://modbase.compbio.ucsf.edu/modloop/ prior to simulation. Modloop predicts the loop conformations by satisfaction of spatial restraints. The program predicts the loop region with good accuracy up to 20 residues. MD simulation was carried out using the program GROMACS version 4.5.5 [11]. The GROMOS96 43a1 force field was used for simulation. The esterase protein was placed in a cubic box with a distance of 3 nm per side from the protein and filled with 52,728 water molecules [single point charge (SPC) model]. A total of 12 Na+ ions were added to neutralize the net negative charge of the whole system, replacing the corresponding number of water molecules, with the aid of

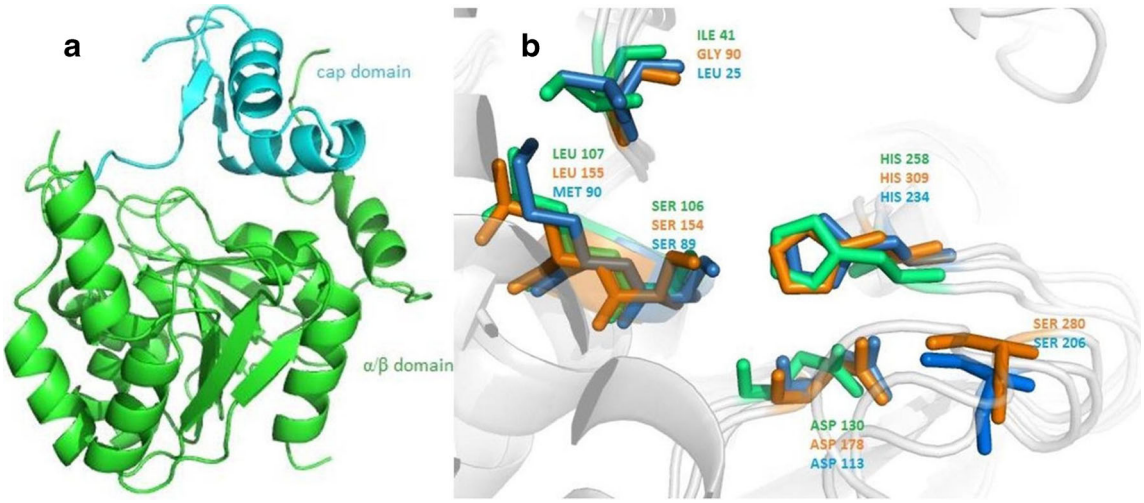

Fig. 1 **a** Cartoon representation of the crystallographic structure of esterase Rv0045c (PDB 3P2M) of *Mycobacterium tuberculosis* showing the two domains. **b** Superposition of the α/β hydrolase domain of Rv0045c, E-2AMS hydrolase (PDB 3KXP) and esterase ybfF (PDB 3BF7) showing a close-up view of the catalytic tetrad residues and the oxyanion hole residues in stick representation. *Orange* Rv0045c, *green* E-2AMS, *blue* ybfF esterase

GROMACS utilities. The system was subjected to energy minimization using the steepest descents method. The equilibrated system was subjected to an all atom MD simulation for 100 ns using periodic boundary conditions. The LINCS algorithm was used to constrain bond lengths using a time step of 2 fs for all calculations. Electrostatic interactions were calculated using the particle mesh Ewald (PME) method. Simulation was performed in the Gibbs ensemble at 300 K and 1 atm using the Berendsen algorithm. Structural analysis of the simulation was performed using built in Gromacs utilities. The cavity volumes were calculated using trj_cavity [12]. The graphs were plotted using xmgrace (http://plasma-gate.weizmann.ac.il/Grace/).The visual analysis of protein structures was carried out using Pymol [9].

Results and discussion

Identification of the catalytic aspartic acid and presence of the catalytic triad

The active site in the α/β hydrolase superfamily usually consists of a catalytic triad containing a nucleophilic serine, a strictly conserved histidine residue and an acidic residue that is usually an aspartic acid or glutamic acid. The active site of Rv0045c, comprising two highly conserved residues Ser154 and His309, was annotated by Zheng et al. [6] through sequence alignment. In the active site, Ser154 acts as a nucleophile and His309 is the catalytic histidine. To find out whether Rv0045c also contains a catalytic triad similar to other α/β hydrolases, we did a structural alignment of Rv0045c with its homologs E-2AMS hydrolase and esterase ybfF. Analysis showed that their active site pockets are similar and the catalytic serine and histidine remained in the same locus (Fig. 1b). As expected, Rv0045c also revealed the presence of a catalytic triad consisting of Ser154, Asp178 and His309, where Asp178 was identified as the third member of the triad.

Asp178 aligned well with the catalytic aspartic acid of E-2AMS and esterase ybfF, Asp178 was found in close proximity to both Ser154 and His309, forming interatomic contacts with them. Sequence alignment fails to identify this acidic residue, probably because of misalignment due to the presence of inserted domains. Due to its polar character, Asp178 forms hydrogen bonds to several residues near the active site, especially the catalytic histidine His309, playing a role not only in catalysis but also in stabilizing the enzyme. The $O^{\delta 1}$ atom of Asp178 interacts with the $H^{\delta 1}$ of His309 as seen in other serine hydrolases. This hydrogen bonding between aspartic acid and histidine plays an important role in the charge-relay system. The results show that Asp178, together with the previously identified Ser154 and His309, constitute the catalytic triad of Rv0045c.

Identification of a putative catalytic tetrad and oxyanion binding site in Rv0045c

Comparative structural study with the homologs also helped identify a putative catalytic tetrad in the active site. A catalytic tetrad has been proposed in some serine proteases and esterases [13, 14]; the tetrad comprises the classical triad and another residue that is involved in structurally stabilizing the catalytic triad. The active site of ybfF esterase consists of a catalytic tetrad consisting of "Ser-His-Asp-Ser" in which Ser206 is another serine other than the nucleophilic Ser89 [13]. Ser280 in Rv0045c aligns to Ser206 in ybfF esterase upon structural superposition (Fig. 1b). Therefore, it is highly likely that the catalytic mechanism in Rv0045c employs a catalytic tetrad system comprising of the catalytic triad Ser-Asp-His and another Ser residue. In the catalytic tetrad, the side chain of the fourth member—Ser/Cys—helps in the stabilization of the standard catalytic triad [14]. The same is observed in Rv0045c, i.e., Ser280 stabilizes Asp178 and His309 through interatomic contacts.

Another important feature in the active site pocket of serine hydrolase is the presence of an oxyanion hole. The position of oxyanion hole residues is well characterized in the structural homologs of Rv0045c, E-2AMS hydrolase and esterase ybfF, by which we identified the location of the oxyanion hole in Rv0045c [15, 13]. In all three structures, the residue adjacent to the catalytic triad serine is one of the residues involved in formation of the oxyanion hole. The oxyanion hole in Rv0045c is found to be formed by the nitrogen atoms of residues Gly90 and Leu155 (Fig. 1b).

Novel member of the HSL family

One of the residues involved in the formation of the oxyanion hole, Gly90, is present within a stack of three glycine residues preceded by a histidine residue forming a His-Gly-Gly-Gly (HGGG) motif—a motif known to be characteristic of HSLs. Multiple sequence alignment with some members of the HSL family, such as *Archaeoglobus fulgidus* carboxylesterase, *Acinetobacter* esterase, *Homo sapiens* HSL, *Pseudomonas* B11-1 lipase, *Ralstonia solancearum* putative esterase/lipase, *M. tuberculosis* Lipy and *M. tuberculosis* Rv1399c showed that the active site residues (Ser154 and His309) and the consensus motif HGGG are conserved in Rv0045c, indicating that Rv0045c is likely a member of the HSL family (Fig. 2). The conservation of the HGGG motif across all the members of HSL indicates the specific role of this motif in the catalytic mechanism of HSLs.

The use of an inhibitor to identify members of the HSL family was proposed by Ben Ali et al. [16]. In vitro enzymatic inhibition studies revealed that all Lip-HSL proteins are inhibited specifically by MmPPOX—an oxadiazolone compound also known as compound 7600 [16]. Molecular

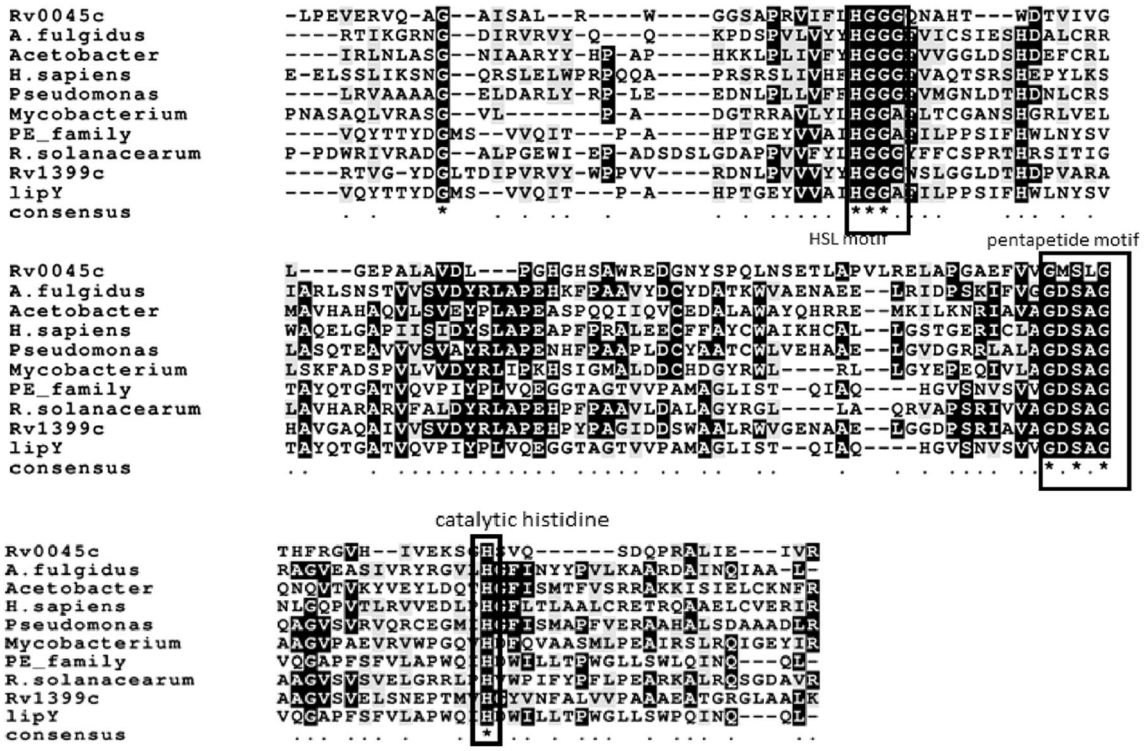

Fig. 2 Multiple sequence alignment of Rv0045c with the other members of the hormone-sensitive lipase (HSL) family showing the conserved HGGG motif and catalytic serine and histidine

docking of MmPPOX with Rv0045c showed that MmPPOX binds to the active site of Rv0045c with a predicted binding energy and theoretical inhibition constant of −5.55 (kcal mol^{-1}) and 86.16 μM, respectively. MmPPOX forms hydrogen bonds with His309 and Ser154 of the catalytic triad and the residues forming the oxyanion hole, Leu155 and Gln92. It also makes hydrophobic interactions with Leu 155, Ile252, and Phe255. Thus, docking results also suggest that Rv0045c is possibly a member of the HSL family (Supplementary Fig. S1). This in silico docking method has its own limitations as it does not take into consideration protein flexibility and solvation effects. However, docking studies provide experimental leads and therefore this finding can be extended to experimental validation to assess the in vivo efficacy of the identified inhibitor.

Molecular dynamics analysis of Rv0045c

A detailed analysis of the MD simulation of Rv0045c revealed that the initial conformation of the structure was in the open state in which the active site residues are accessible to the solvent and the active site pocket is exposed for allowing the substrate to bind. We calculated the root mean square deviation (RMSD) and radius of gyration from the initial structure to measure the convergence of the protein system, as shown in Supplementary Fig S2a,b. The RMSD of Rv0045c reaches equilibrium at about 25 ns and attains a value of 0.5 nm. The radius of gyration undergoes great fluctuation, it decreases initially up to 25 ns and later fluctuates until it attains stability at around 70 ns. The high fluctuation in the radius of gyration and relatively large RMSD value of 5 Å indicates that the protein is undergoing significant structural transition. After carefully visualizing the MD, it was found that the protein undergoes a transition from open to closed conformation by 43 ns. The active site cavity remains closed and inaccessible until 53 ns and slowly transforms to a semi open/semi closed state and remains in the same conformation from 59 to 66.7 ns. In the last 20 ns we find that the mouth of the active site pocket transits frequently between closed to a very narrow open cavity. This transition from open to closed and later to a semi open/semi closed state was analyzed quantitatively by calculating the cavity volumes. The time evolution of cavity volumes throughout the trajectory can be seen in Supplementary Fig S3 .The active site cavity increases initially up to 20 ns from 1,500 $Å^3$ to 2,800 $Å^3$ and decreases by almost 1,600 $Å^3$ when it goes to a closed state at 43 ns; again during the transition to the semi-closed state at 63 ns we see an increase and decrease in the active site pocket. From the MD simulation, we were able to see the transition from open to closed state (Supplementary Movie S1) and later to a semi open state.

Structural rearrangements leading to conformational transition from open to closed state

Our MD analysis revealed three prominent structural rearrangements taking place during the closing mechanism (until 45 ns); the conformational change involves domain reorientation accompanied by loop motions and histidine flipping (Supplementary Fig. S4). The root mean square fluctuation (RMSF) captures, for each atom, the fluctuation about its average position, which gives insight into the flexibility of regions in the protein. The RMSF calculated for the entire 100-ns-long trajectory shows that the loops surrounding the active site pocket and the loops connecting the antiparallel beta sheet in the cap and alpha beta domain are highly mobile and have RMSF >2 Å (Supplementary Fig. S2c). The highly fluctuating loop encompassing residues 190–205 and the three adjacent loops formed by residues 221–225, residues 278–284 and residues 305–310 surrounding the active site may play an important role in gating the enzyme. Their coupled motion significantly reduced the active site cavity, thereby decreasing the radius of gyration and closing the active site pocket (Supplementary Fig. S5). To obtain a quantitative view of active site closure, we plotted the interatomic distances between the Cα atoms of the amino acids from each domain (Supplementary Fig. S6). It was seen that the highly flexible mobile loop 190–205 undergoes a complete rearrangement, with a maximum displacement of 20 Å closing the active site cavity. The movement of these four loops towards closing the active site pocket can be visualized in Supplementary Movies S1 and S2.

Another important change that takes place during the closing mechanism is that the inter-domain distance between the cap domain and the alpha beta domain is greatly reduced. This results in formation of new interatomic hydrogen bonding interactions between the cap domain and alpha beta domain in the closed state that are not present in the initial conformation. The cap domain forms hydrogen bonds with residues 305–307 and 312–318 of the alpha beta domain; the interactions between the residues of the two domains are tabulated in Supplementary Table S1. The cap domain plays an important role in the opening and closing mechanism of the active site pocket.

Role of the mobile catalytic histidine in the ring flipping mechanism

From a visual analysis of the simulation trajectories, we find that the catalytic histidine is mobile during the transition from open to closed and to the semi-open state, which is also evident from the RMSD of histidine (Fig. 3a). The imidazole ring rotates and shifts almost in the opposite direction; this rotation movement was captured by measuring the dihedral angle for CA-CB-CG-CD2 of His309 (Fig. 3c). This movement of the imidazole ring of histidine happens twice during the 100 ns simulation. In the open conformation, the imidazole ring is directed downwards towards the active site lumen in close proximity to the serine residue, forming a hydrogen bond between the $N^{\varepsilon 2}$ of His309 with the O^{γ} of Ser154 (Fig. 3b). During transition to the closed state, we find that the imidazole ring undergoes a ring flip of almost 180° resulting in an increase in the distance between the O^{γ} atom of serine and the $N^{\varepsilon 2}$ atom of histidine and bringing it to an angle that is less favorable for hydrogen bonding interaction. Further, during the change in the conformation from closed to semi open state around 70 ns, the imidazole ring again undergoes a ring flip and interacts with the O atom of the oxyanion hole residue Gly90 (Fig. 3e).

Our observations are consistent with the histidine ring-flipping hypothesis. A catalytic mechanism involving the directed movement of the imidazole ring of the active site histidyl residue was proposed in the histidine ring flipping model [17]. According to this model, the ring flip of catalytic histidine is required for histidine to act both as a general base (in the formation of the first tetrahedral intermediate) and as an acid (donating a proton to the substrate leaving group to promote formation of the acyl enzyme) [18]. In the first step of the catalytic mechanism, a neutral His309 $N^{\varepsilon 2}$ is positioned to abstract the proton from Ser O^{γ} whereas, during the formation of the acyl enzyme complex, histidine ring flipping is necessary to preferentially position His309 $N^{\varepsilon 2}$ to promote protonation of the leaving group and to prevent back protonation of serine. The movement of the histidine ring can be visualized in Supplementary Movie S3.

Conformational transitions in terms of the catalytic mechanism

Conformational dynamics are a major requisite for enzyme function. There is increasing data to support the view that free enzyme dynamics intrinsically encompass all the conformations necessary for substrate-binding, transition state stabilization and product release [19–21]. Hydrogen bonding interactions between catalytic residues play a crucial role in the charge–relay system, and they change between different stages of catalysis. There is a complex network of H-bonds between active site residues that is seen to fluctuate as a function of time in the simulation. The current study is a free enzyme simulation of Rv0045c esterase without substrate. We studied changes in the hydrogen-bonding interactions between the catalytic and oxyanion hole residues and found that the free enzyme simulation mimics the different stages of catalysis (Fig. 4). The catalytic mechanism of serine esterases is well studied and the hydrogen bonding interactions between the active site residues and oxyanion hole during each sub stage is known [22, 23], thus providing a platform for our analysis.

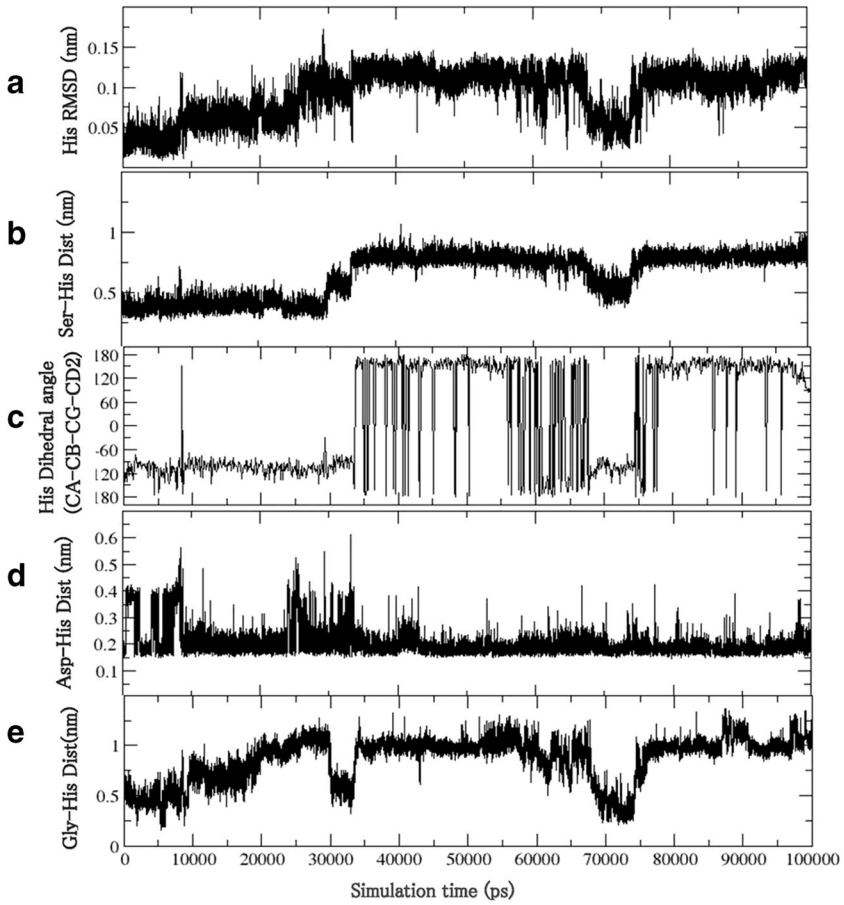

Fig. 3 Time dependent changes in the catalytic histidine

We saw that the initial conformation of the enzyme Rv0045c is open to allow the substrate to enter the active site cavity. In Rv0045c, we found that, in the initial stage of the simulation, His309 $N^{\varepsilon 2}$ is hydrogen bonded to Ser154 O^{γ} and His309 $N^{\delta 1}$ to Asp178 to facilitate the formation of the tetrahedral intermediate. His309 $N^{\varepsilon 2}$ of the imidazole ring is positioned in such a way that it can abstract the proton from the Ser154 O^{γ} as seen in Fig. 4 stage 1; within a few nanoseconds the Ser–His hydrogen bond is lost and the oxyanion hole residues interact with the Ser154 O^{γ} with their backbone nitrogen atoms (Fig. 4, stage 2). Hydrogen bond interactions between the oxyanion hole residues Gly90 NH and Leu155 NH with Ser154 O^{γ} would help provide electrophilic assistance, which would enhance the polarization of the bond, aiding the attack of Ser154 O^{γ}. The function of oxyanion hole residues is to interact with the tetrahedral intermediate formed and stabilize it.

We discussed earlier that the catalytic histidine is highly mobile and undergoes a ring flip. Conformational change involving the histidine ring flip would have to take place after the first proton transfer from Ser154 O^{γ} to His309 $N^{\varepsilon 2}$, i.e., after the initial formation of the tetrahedral intermediate. We see that the hydrogen bonding interaction of Asp178 and Ser280 helps to orient the histidine imidazole ring towards the flipped conformation (Fig. 4, stage 3). After the histidine flipping event, the interaction between Asp178 and Ser280 is not as stable, suggesting that this serine in the tetrad plays an important part in reorientation of the histidine. Our simulation results mimic the tetrahedral intermediate-bound state at this stage (Fig. 4, stage 4), during which we also observe that the active site pocket is completely occluded (44–53 ns), which leaves no gate for substrate entry. In the closed state, during the flipped conformation we see that the His309 $N^{\varepsilon 2}$ is free to form a hydrogen bonding interaction if the tetrahedral intermediate was formed, His309 $N^{\varepsilon 2}$ is preferentially positioned not only to promote protonation of the leaving group but also to prevent back protonation of serine (Fig. 4, stage 4). As per the general catalytic mechanism, the tetrahedral intermediate would collapse, assisted by His309-H^{+} acting as a general acid to yield the acylenzyme intermediate [22]. Thus, the formation and collapse of the first tetrahedral intermediate involves proton shuttle from Ser154 O^{γ} to His309 $N^{\varepsilon 2}$ and finally to the leaving group. The leaving group has to be expelled, for which the active site cavity has to open. We see that, after 53 ns, the active site cavity changes to a semi open state, probably to expel this leaving group.

After a few nanoseconds (near 60 ns), we find that the His $N^{\varepsilon 2}$ forms a hydrogen bond with a water molecule as seen in

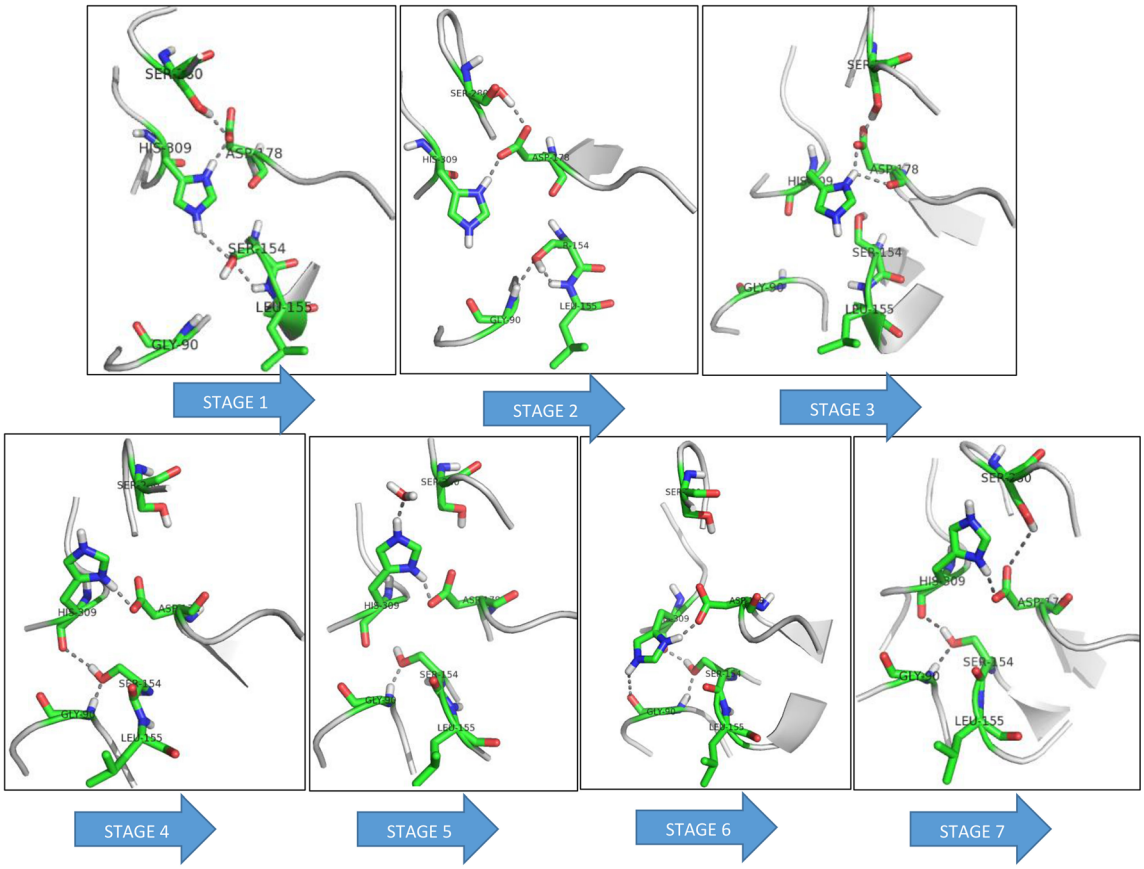

Fig. 4 Structural snapshots of the changes in hydrogen bonding interactions within the active site cavity mimicking the different stages in catalysis. Key residues (Ser154, Asp178, His309, Ser280, Gly90 and Leu155) are shown in stick representation

Fig. 4, stage 5. This water molecule probably substitutes for the hydrolytic water. In some crystallographic studies, water molecules that were suggested to be this "hydrolytic water molecule" because they seemed to be in the favorable position have been observed. It is suggested that the hydrolytic water should approach the acylenzyme from the leaving group side of the active site and form a hydrogen bond with the catalytic histidine [24]. The same is observed in the simulation; we observe that a water molecule enters from outside the active site cavity and forms a hydrogen bond with the His309 $N^{\varepsilon 2}$. The hydrolytic water plays a crucial role in the deacylation reaction during catalysis as it triggers the breakdown of acylenzyme to form a second tetrahedral intermediate [22].

During the next conformational transition in the simulation (70–74 ns), we see that the histidine ring flips back into a different orientation and His309 $N^{\varepsilon 2}$ interacts with the Gly90 (Fig. 4, stage 6; Fig. 3e). The base that accepts the proton from the catalytic water molecule during deacylation has to transfer it to the Ser154 O^{γ} in order to regenerate the active site. It is possible that His assists in the deacylation by providing a means to transfer the proton to Ser154 O^{γ} through Gly90. While histidine interacts with Gly90, we also find a hydrogen bonding interaction of Ser154 O^{γ} to the NH of Gly90. Based on these observations, we hypothesize that histidine shuttles the proton back to the serine by means of Gly90. In the final stage of the reaction, the second tetrahedral intermediate collapses, expelling the product. The final 25 ns of the simulation has a stable set of interactions inside the active site pocket and the conformation fluctuates between the semi open and the closed state (Fig. 4, stage 7).

At all stages, the oxyanion and catalytic triad function cooperatively, and the interaction between the Asp178 and His309 is maintained throughout the simulation (Fig. 3d). With the help of MD simulations we can see that, in the absence of the substrate, the free enzyme mimics the different stages of catalysis, which correlates with the conformational transitions observed in the active site cavity. This result supports the proposal that the substrate-free enzyme possesses an innate ability to interconvert between the different states in the reaction mechanism. The same can probably be observed in other lid-gated enzymes as they have both open and closed conformations in equilibrium before ligand binding [25]. Substrate-free enzyme mimicking catalytic stages was observed experimentally earlier in prolyl cis–trans isomerase cyclophilin A (CypA) by NMR relaxation experiment. The enzyme motions detected during catalysis were observed in the free enzyme state with frequencies corresponding to the catalytic turnover rates [26].

Summary

In the current study, using computational approaches we have putatively identified the residues forming the oxyanion hole and catalytic tetrad of the active site of the esterase Rv0045c. Our studies also reveal that Rv0045c is a possible member of the HSL family. Ours is the first attempt to observe the dynamic behavior of the esterase Rv0045c. The predisposition of Rv0045c to undergo major functionally related conformational changes was investigated through extensive MD simulations of the free enzyme for 100 ns. The structural changes involved in open to closed state transitions of Rv0045c have been described. The conformational change involving the imidazole ring supports the histidine ring-flipping hypothesis. Finally, from analysis of the changing hydrogen bonding interactions between residues in the active site pocket, we find that the substrate-free simulation of Rv0045c mimics the different stages in catalysis.

Acknowledgment The authors thank the Biotechnology Information System (BTIS), Department of Biotechnology for computational facilities.

References

1. Brockerhoff H (2012) Lipolytic enzymes. Elsevier, Amsterdam
2. Hemila H, Koivula TT, Palva I (1994) Hormone-sensitive lipase is closely related to several bacterial proteins, and distantly related to acetylcholinesterase and lipoprotein lipase: identification of a superfamily of esterases and lipases. Biochim Biophys Acta Lipids Lipid Metab 1210:249–253. doi:10.1016/0005-2760(94)90129-5
3. Schweiger M, Schreiber R, Haemmerle G, Lass A, Fledelius C, Jacobsen P et al (2006) Adipose triglyceride lipase and hormone-sensitive lipase are the major enzymes in adipose tissue triacylglycerol catabolism. J Biol Chem 281:40236–40241. doi:10.1074/jbc.M608048200
4. Bornscheuer UT, Kazlauskas RJ (2006) Lipases and esterases: sections 5.3-5.4. Wiley-VCH, Weinheim, pp 141–183
5. Guo J, Zheng X, Xu L, Liu Z, Xu K, Li S et al (2010) Characterization of a novel esterase Rv0045c from Mycobacterium tuberculosis. PLoS One 5:e13143. doi:10.1371/journal.pone.0013143
6. Zheng X, Guo J, Xu L, Li H, Zhang D, Zhang K et al (2011) Crystal structure of a novel esterase Rv0045c from Mycobacterium tuberculosis. PLoS One 6:e20506. doi:10.1371/journal.pone.0020506
7. Morris GM, Goodsell DS, Huey R, Lindstrom W, Hart WE, Kurowski S et al (2010) AutoDock v4. 2. http://autodock.scripps.edu/
8. Hekkelman ML, te Beek TA, Pettifer SR, Thorne D, Attwood TK, Vriend G (2010) WIWS: a protein structure bioinformatics Web service collection. Nucleic Acids Res 38:W719–W723. doi:10.1093/nar/gkq453
9. DeLano WL (2002) The PyMOL molecular graphics system. DeLano Scientific, Palo Alto, CA. http://www.pymol.org
10. Fiser A, Sali A (2003) ModLoop: automated modeling of loops in protein structures. Bioinformatics 19(18):2500–2501. doi:10.1093/bioinformatics/btg362
11. Hess B, Kutzner C, Van Der Spoel D, Lindahl E (2008) GROMACS 4: algorithms for highly efficient, load-balanced, and scalable molecular simulation. J Chem Theory Comput 4:435–447. doi:10.1021/ct700301q
12. Teresa P, Alexandra E, Diana G, Martin BU, Peter JP (2014) Efficient characterization of protein cavities within molecular simulation trajectories: trj_cavity. J Chem Theory Comput 10(5):2151–2164. doi:10.1021/ct401098b
13. Park SY, Lee SH, Lee J, Nishi K, Kim YS, Jung CH, Kim JS (2008) High-resolution structure of ybfF from *Escherichia coli* K12: a unique substrate-binding crevice generated by domain arrangement. J Mol Biol 376:1426–1437. doi:10.1016/j.jmb.2007.12.062
14. Krem MM, Di Cera E (2001) Molecular markers of serine protease evolution. EMBO J 20:3036–3045. doi:10.1093/emboj/20.12.3036
15. McCulloch KM, Mukherjee T, Begley TP, Ealick SE (2010) Structure determination and characterization of the vitamin B6 degradative enzyme (E)-2-(acetamidomethylene) succinate hydrolase. Biochemistry 49:1226–1235. doi:10.1021/bi901812p
16. Ben Ali Y, Chahinian H, Petry S, Muller G, Lebrun R, Verger R et al (2006) Use of an inhibitor to identify members of the hormone-sensitive lipase family. Biochemistry 45:14183–14191. doi:10.1021/bi0613978
17. Ash EL, Sudmeier JL, Day RM, Vincent M, Torchilin EV, Haddad KC et al (2000) Unusual 1H NMR chemical shifts support (His) Cε 1—H···O== C H-bond: proposal for reaction-driven ring flip mechanism in serine protease catalysis. Proc Natl Acad Sci USA 97:10371–10376. doi:10.1073/pnas.97.19.10371
18. Bachovchin WW (1986) Nitrogen-15 NMR spectroscopy of hydrogen-bonding interactions in the active site of serine proteases: evidence for a moving histidine mechanism. Biochemistry 25:7751–7759. doi:10.1021/bi00371a070
19. Ma B, Nussinov R (2010) Enzyme dynamics point to stepwise conformational selection in catalysis. Curr Opin Chem Biol 14:652–659. doi:10.1016/j.cbpa.2010.08.012
20. Pentikäinen U, Pentikäinen OT, Mulholland AJ (2008) Cooperative symmetric to asymmetric conformational transition of the apo-form of scavenger decapping enzyme revealed by simulations. Proteins: Struct Funct Bioinf 70(2):498–508. doi:10.1002/prot.21540
21. McGeagh JD, Ranaghan KE, Mulholland AJ (2011) Protein dynamics and enzyme catalysis: insights from simulations. Biochim Biophys Acta Proteins Proteomics 1814(8):1077–1092. doi:10.1016/j.bbapap.2010.12.002
22. Hedstrom L (2002) Serine protease mechanism and specificity. Chem Rev 102(12):4501–4524. doi:10.1021/cr000033x
23. Dodson G, Wlodawer A (1998) Catalytic triads and their relatives. Trends Biochem Sci 23(9):347–352. doi:10.1016/S0968-0004(98)01254-7
24. Perona JJ, Craik CS, Fletterick RJ, Singer PT (1993) Locating the catalytic water molecule in serine proteases. Science 261:620–620. doi:10.1126/science.8342029\
25. Hammes GG, Chang YC, Oas TG (2009) Conformational selection or induced fit: a flux description of reaction mechanism. Proc Natl Acad Sci USA 106(33):13737–13741. doi:10.1073/pnas.0907195106
26. Eisenmesser EZ, Millet O, Labeikovsky W, Korzhnev DM, Wolf-Watz M, Bosco DA, Kern D (2005) Intrinsic dynamics of an enzyme underlies catalysis. Nature 438(7064):117–121. doi:10.1038/nature04105